PHYSICAL REVIEW B **67**, 054108 (2003)

Wafer curvature in molecular beam epitaxy grown heterostructures

T. Dieing* and B. F. Usher
Department of Electronic Engineering, La Trobe University, Victoria 3086, Australia

(Received 15 April 2002; revised manuscript received 15 July 2002; published 28 February 2003)

Wafer curvature in strained molecular beam epitaxy grown heterostructures has been studied. Theories on semiconductor wafer curvature have been re-examined and errors that have persisted in the literature have been corrected. This paper presents an approach to calculating the wafer curvature for an arbitrary multilayer system using basic physical equations. X-ray diffraction measurements have been performed to measure the radius of curvature of several samples and the results are in good agreement with the theory presented here.

DOI: 10.1103/PhysRevB.67.054108 PACS number(s): 81.05.Ea, 68.65.−k, 81.15.Hi

I. INTRODUCTION

X-ray diffraction represents one of the most commonly used methods for the structural characterization of single and multiple heterostructures. Bending of these wafers can cause a smearing of the x-ray spectrum and fine thickness fringes may not be seen anymore. This effect has recently been observed during 90° Bragg reflection measurements performed at the European Synchrotron Radiation Facility (ESRF) and the Advanced Photon Source synchrotron facility (APS).[1] A significant degradation of the data collected was related to the bending of the structures used. The molecular beam epitaxy (MBE) grown structures were soldered onto a heater block using indium, which most likely was responsible for this strong curvature.

In situ measurements of wafer curvature during MBE,[2] and metalorganic chemical vapor deposition (MOCVD)[3,4] growth as well as *ex situ* measurements[5,6] demonstrate that by measuring the radius of curvature valuable structural information on strained layers can be obtained. However, most studies directly or indirectly used an equation obtained by Stoney[7] in 1909, which was applied to the case of electrolytically deposited metallic films and does not hold for semiconductor heterostructures with coherent interfaces.

This demonstrates the necessity for a clear description of these bending effects. Therefore a new theoretical description has been developed, based on a two-dimensional model of a heterostructure. The first part of this paper introduces this model before it is shown how the radius of curvature for a single-layer system can be calculated. The description is then generalized to develop an expression, which describes an arbitrary multilayered heterostructure. X-ray diffraction measurements using a double crystal x-ray setup have been performed on several samples to detect the radius of curvature and the results are in agreement with the theory introduced.

II. THEORY

A. Grid structure and strain in epitaxial layers

Growing epitaxial layers that are not lattice matched to a substrate causes the bonds in the layers to be strained. The bonds in the substrate are, although to a lesser degree, strained as well and so the unit cells throughout the wafer are distorted. For the present case it is assumed that the layer's natural lattice constant is larger than the substrate's as it is for the case of a GaAs substrate and an $\mathrm{In}_x\mathrm{Ga}_{1-x}\mathrm{As}$ layer; however, the results are readily generalized. It is assumed that the bending can be approximated as a cylindrical bending and therefore a two-dimensional treatment is performed rather than a complete three-dimensional treatment which would be required to describe spherical bending. However by taking into account the biaxial strain, the three-dimensional case is largely included and the treatment here will be sufficient. The benefit of the cylindrical treatment is that the parallel lattice constant $d_\parallel$ will change linearly with position as can be seen in Fig. 1. The atoms within the wafer line up and the extensions of these lines converge to a point as shown in Fig. 1.

In the case of an epitaxial structure consisting of an $\mathrm{In}_x\mathrm{Ga}_{1-x}\mathrm{As}$ layer grown on a GaAs substrate, the bonds in the interfacial plane are compressed and the strain will be negative. At the neutral plane the substrate's lattice constant is unchanged whereas it is stretched above and compressed below the neutral plane showing negative and positive

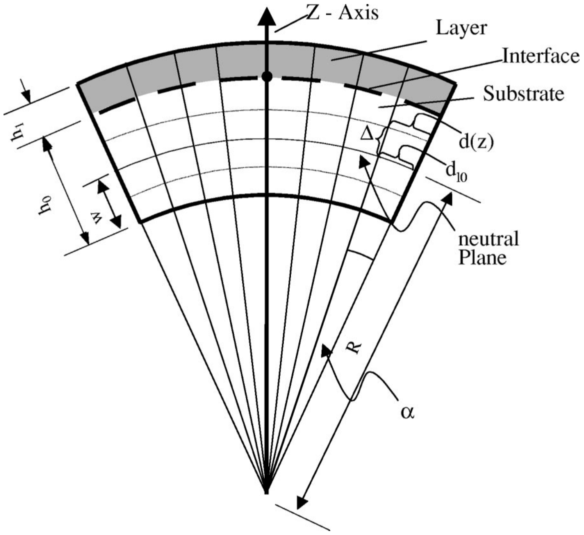

FIG. 1. The thickness of the substrate in this curved composite is h_0 and the thickness of the layer is h_1. R is the radius of curvature of the structure; w is the distance from the neutral plane to the bottom of the substrate, d_{l0} is the natural lattice constant of the substrate, which is at the position of the neutral plane, and $d(z)$ is the parallel lattice constant for any value of z. The z axis has its origin at the interface.

0163-1829/2003/67(5)/054108(8)/$20.00

strains, respectively. The lattice constants can be expressed in terms of the radius of curvature R and α, the angle subtending the unit cell as

$$d_{l0} = R \cdot \alpha, \tag{1}$$

$$d(z) = (R + \Delta) \cdot \alpha \tag{2}$$

where d_{l0} represents the natural lattice constant of the substrate at the neutral plane and $d(z)$ is the lattice constant at a positive distance Δ above the neutral plane. Here a positive radius of curvature represents convex bending as shown in Fig. 1 and a negative radius of curvature represents concave bending. Introducing the z axis with its origin $(z=0)$ at the interface Δ can be replaced by $z + (h_0 - w)$ since the neutral plane is at the position $z = -(h_0 - w)$ and thus the z position of Δ can be expressed as $z = \Delta - (h_0 - w)$. Using this relationship $d(z)$ can be expressed as $d(z) = (R + z + h_0 - w) \cdot \alpha$. Solving Eq. (1) for α and substituting it in the expression for $d(z)$ leads to

$$d(z) = d_{l0} \cdot \left(1 + \frac{z + h_0 - w}{R}\right), \tag{3}$$

which describes the parallel lattice constant for all z whether in the substrate or in the layer. From this the parallel or in-plane strain can be calculated from the definition

$$\varepsilon^{\parallel} = \frac{d - d_0}{d_0}, \tag{4}$$

where d_0 is the natural lattice constant and d the lattice constant of the strained lattice in the parallel direction. Using $d(z)$ for d and the substrate's natural lattice constant d_{l0} for d_0 leads to an expression for the parallel strain in the substrate as a function of z, which is

$$\varepsilon_0^{\parallel}(z) = \frac{z + h_0 - w}{R}, \tag{5}$$

where w again is the distance between the neutral plane and the bottom of the substrate.[8] Following the steps above for the layer using the lattice constant $d(z)$ for d and the layer's natural lattice constant d_{l1} for d_0 results in

$$\varepsilon_1^{\parallel}(z) = \frac{d_{l0}}{d_{l1}} \cdot \left(1 + \frac{z + h_0 - w}{R}\right) - 1 = \frac{d_{l0}}{d_{l1}} \cdot [1 + \varepsilon_0(z)] - 1, \tag{6}$$

where d_{l1} can be calculated using Vegard's Law. If, however, the layer contains misfit dislocations we recommend the use of a so-called effective lattice constant as proposed by Chu *et al.*,[9] and given by

$$d'_{l1} = d_{l1} + \frac{N_1 - N_0}{N_0} \cdot b_I \tag{7}$$

where d'_{l1} represents the effective lattice constant, d_{l1} the lattice constant as calculated using Vegard's Law, N_1 and N_0 are the number of atoms along each side of the interface between the layer and the substrate, respectively, and b_I is the component of the Burgers vector along the interface. This effective lattice constant should then be used instead of d_{l1} for all the following calculations.

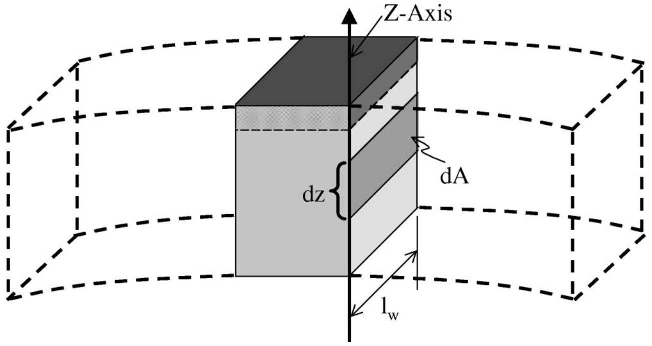

FIG. 2. Part of the curved wafer showing the area dA, the wafer's depth l_w, and the fragment dz.

If there are significant differences in the thermal expansion coefficients of the layer and the substrate, all the lattice constants should be recalculated according to $d_{li,th} = d_{li} \cdot (1 + \alpha_i \cdot T)$ where d_{li} represents the lattice constant of the substrate (d_{l0}) or of one of the layers. α_i is the thermal expansion coefficient of the substrate or layer and T is the temperature in Kelvin.

For a typical dislocation free $\mathrm{In}_x\mathrm{Ga}_{1-x}\mathrm{As}/\mathrm{GaAs}$ structure with x=0.5% and a layer thickness of 0.5 μm grown on a 400-μm-thick substrate, the strain at the interface jumps from slightly positive values $(\approx +0.0002\%)$ in the substrate just below the interface, to much higher, but negative values $(\approx -0.036\%)$ in the layer just above the interface.

B. Neutral plane

The neutral plane, as we define it here, describes the position of the horizontal plane where the lattice constant $[d(z)$; see Eq. (3)] equals the natural lattice constant of the substrate (d_{l0}). The radius of curvature is measured relative to this plane. For most of the structures commonly grown by MBE this neutral plane will be situated within the substrate describing the horizontal position where the substrate is unstrained. An unbent substrate without any layer grown onto it will, however, have its natural lattice constant at every horizontal position within the substrate, and therefore the neutral plane cannot be assigned to a specific position. Since we are looking at a static model, the sum of the forces in the structure pulling to the right and to the left of, for example, the z axis must equal 0. From this sum it is possible to determine the position of the neutral plane. The forces can be calculated using the stresses s at each point according to

$$F = \int dF = \int \sigma \cdot dA, \tag{8}$$

where dA represents a small area, which can be replaced by the depth of the wafer l_w multiplied by dz. The strain can be expressed as $\sigma = E \cdot \varepsilon$ using Hooke's law. It is assumed that the stresses are biaxial, i.e., that the in-plane forces dF perpendicular to the depth of the wafer (l_w; see Fig. 2), are the same as those parallel to l_w.

Furthermore the layer in the *z* direction is considered to be unconstrained, and therefore the stress in the direction of the *z* axis is zero. Therefore, Poisson's ratio (ν) must be used. Young's Modulus in Hooke's law may then be replaced by the elastic constant E^*, where $E^* = E/(1-\nu)$. Therefore Eq. (8) becomes

$$F = E^* \cdot l_w \cdot \int \varepsilon dz. \tag{9}$$

The integration of Eq. (9) can now be performed for the substrate from $z = -h_0$ to $z = 0$, using the elastic constant of the substrate E_0^* and the strain in the substrate [Eq. (5)] and also for the layer between the boundaries $z = 0$ and $z = h_1$, using the elastic constant E_1^* of the layer and the strain in the layer [Eq. (6)]. This results in

$$F_0 = E_0^* \cdot l_w \cdot \frac{h_0}{R} \cdot \left(\frac{h_0}{2} - w \right), \tag{10}$$

$$F_1 = E_1^* \cdot l_w \cdot \int_{z=0}^{z=h_1} \left[\frac{d_{l0}}{d_{l1}} \cdot \left(1 + \frac{z + h_0 - w}{R} \right) - 1 \right] dz \tag{11}$$

for the substrate and layer, respectively. Summing these forces to zero and solving for *w*, the position of the neutral plane, leads to

$$w = \frac{h_0}{2} + \frac{E_1^* \cdot h_1 \cdot \frac{1}{d_{l1}} \cdot \left[h_0 + h_1 + 2 \cdot R \cdot \left(1 - \frac{d_{l1}}{d_{l0}} \right) \right]}{2 \cdot \left(E_0^* \cdot h_0 \cdot \frac{1}{d_{l0}} + E_1^* \cdot h_1 \cdot \frac{1}{d_{l1}} \right)}. \tag{12}$$

An almost equivalent description of the position of the neutral plane was given by Davidenkov,[10] except that his treatment was for electrolytically deposited materials. In that case the different strains in the layer and in the substrate due to the different natural lattice constants were not considered. This is the same as if d_{l1} equaled d_{l0} in Eq. (12). Chu *et al.*[9] as well as Noyan *et al.*[11] used Davidenkov's expression, which is incorrect for epitaxial layers, to describe the radius of curvature of layered semiconductor structures. Townsend *et al.*[12] presented another approach for the description of curvature as well as the position of the neutral plane, but again the fact that for epitaxial layers with a coherent interface the atoms will line up vertically as shown in Fig. 1 is neglected.

For very thin layers, the second term in Eq. (12), which contains the product of a large radius and a small layer thickness, can be approximated by $-h_0/6$. Thus, if the layer is very thin and the layer's lattice constant is similar to that of the substrate, *w* then approaches $h_0/3$ (see Appendix A). This can be explained by the fact that, before growing any layer the substrate is, in the ideal case, not bent at all. This means that the radius *R* is infinite and the thickness of the layer h_1 is 0. The product of h_1 and *R* can then take any value. One may say that either the neutral plane does not exist in this case, or that it is everywhere. Though neglecting the different lattice constants of the substrate and the layer in the equation describing the position of the neutral plane, Townsend *et al.* found the position of the neutral plane as well at one-third of the substrate height if their equation is approximated for the thin layer case. Stoney concluded, as well, that the neutral plane is situated at this position, although in his solution the neutral plane would not move with increasing layer thickness.

If the layer's lattice constant and the elastic constants are, however, the same as that of the substrate and there are external forces bending the structure ($R \neq \infty$), the position of the neutral plane will be equal to $(h_0 + h_1)/2$ which is half the overall height of the structure. This result for uniform materials is widely described in the literature.[13,14]

C. Radius of curvature

To determine the radius of curvature of an epitaxial structure, the total mechanical strain energy of the structure, including the effects of bending, is calculated. The radius *R* is the radius for which this energy is a minimum. The mechanical strain energy of a structure can be defined as

$$dW = dV \cdot \int \sigma(\varepsilon) d\varepsilon. \tag{13}$$

The volume dV equals $[d_x(z) \cdot d_y(z)] dz(z)$, and since

$$d_x(z) = d_y(z) = d(z) = d_{l0} \cdot [1 + \varepsilon_0^{||}(z)],$$

$$dz(z) = dz \cdot \left[1 - \frac{2 \cdot \nu}{1 - \nu} \cdot \varepsilon_0^{||}(z) \right],$$

the volume can be expressed in terms of the strain $\varepsilon_0^{||}(z)$ as

$$\begin{aligned} dV &= d_{l0}^2 \cdot [1 + 2 \cdot \varepsilon_0^{||}(z) + \varepsilon_0^{||2}(z)] \cdot \left[1 - \frac{2 \cdot \nu}{1 - \nu} \cdot \varepsilon_0^{||}(z) \right] dz \\ &= d_{l0}^2 \cdot \left[1 + \underline{\frac{2 - 4 \cdot \nu}{1 - \nu} \cdot \varepsilon_0^{||}(z) + \frac{1 - 5 \cdot \nu}{1 - \nu} \cdot \varepsilon_0^{||2}(z) - \frac{2 \cdot \nu}{1 - \nu} \cdot \varepsilon_0^{||3}(z)} \right] dz. \end{aligned} \tag{14}$$

Calculating the total energy of coherent structures using Eq. (14) in Eq. (13) and determining the radius of curvature via the minimization of this energy, shows that the underlined terms of Eq. (14) only have a minor effect on the radius of curvature. The relative difference of the radii of curvature when including and omitting these terms is $<0.4\%$. For incoherent structures with layer thicknesses up to 20 times the thicknesses of coherent structures this difference increases but will still not exceed 1.3%. The fact that the strain $\varepsilon_0^{||}(z)$ for these structures always stays below $\approx 0.002\%$ and therefore the underlined terms do not exceed 2×10^{-5} shows that the volume dV can be reasonably approximated as $dV = d_{l0}^2 dz$ for mathematical convenience. Using Hooke's law, the integral in Eq. (13) can then be performed between the boundaries 0 and $\varepsilon(z)$ to obtain an equation showing the dependence of the energy on z and the strain $\varepsilon(z)$ at this position. Furthermore, the Young's moduli are replaced by the elastic constants (E_0^* and E_1^*) as seen above. As the strain itself depends on z, the energy can be renamed $dW(z)$, so that

$$dW(z) = \tfrac{1}{2}\cdot d_{l0}^2 \cdot E^* \cdot [\varepsilon(z)]^2 dz. \tag{15}$$

Integrating this equation for the substrate and for the layer using appropriate boundary conditions, elastic constants and strains, the mechanical strain energy in the layer and in the substrate can be found. Replacing w, the position of the neutral plane from Eq. (12) and adding these energies leads to the total mechanical strain energy in the structure as

$$\begin{aligned} W = \frac{d_{l0}^3}{2\cdot R^2}\cdot \Bigg\{ & P_0 \cdot \left[\frac{1}{12}h_0^2 + \frac{1}{4}\left(\frac{P_1\cdot(h_0+h_1+2\cdot d_1\cdot R)}{P_1+P_0}\right)^2\right] \\ & + P_1 \cdot \frac{d_{l0}}{d_{l1}} \cdot \left[\frac{1}{12}h_1^2 + \frac{1}{4}\left(\frac{P_0\cdot(h_0+h_1+2\cdot d_1\cdot R)}{P_1+P_0}\right)^2\right]\Bigg\}. \end{aligned} \tag{16}$$

where the following substitutions have been made:

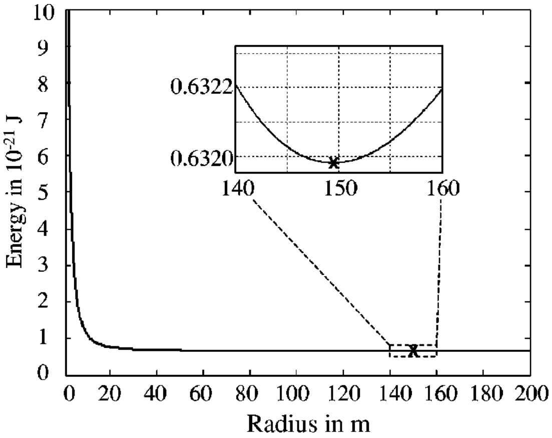

FIG. 3. Energy as a function of the radius of curvature for a 400 μm thick GaAs substrate with a 0.5-μm $In_{0.005}Ga_{0.995}As$ layer.

$$P_0 = \frac{E_0^* \cdot h_0}{d_{l0}}, \quad P_1 = \frac{E_1^* \cdot h_1}{d_{l1}} \quad \text{and} \quad d_1 = 1 - \frac{d_{l1}}{d_{l0}}. \tag{17}$$

Figure 3 shows the dependence of the total mechanical energy W on the radius R. For this calculation the Young's modulus of GaAs (8.53×10^{10} N/m^2) (Ref. 15) was used and it was assumed that the Young's moduli of the layer and the substrate were identical. This is reasonable because Young's moduli for GaAs and InAs are quite similar and since Young's modulus of the layer is expected to be approximately linear with the Indium fraction in the layer, it is clear that the Young's moduli will be almost identical. The literature value for Poisson's ratio of GaAs (0.312) (Ref. 16) was used for both the layer and the substrate. While the plot of W versus R does not at first appear to exhibit a minimum, the points **X** in Fig. 3 indicate the energy does have a minimum. Here the radius of curvature is 149.5 m for a structure consisting of a 0.5-μm $In_{0.005}Ga_{0.995}As$ layer on a 400-μm-thick GaAs substrate. The radius where the energy takes its minimal value can be calculated by setting the derivative of Eq. (16) with respect to R equal to zero and solving the equation for R. Then

$$R = -\frac{h_0+h_1}{2\cdot d_1}\cdot\left[1+\frac{1}{3}\cdot\frac{(P_0\cdot h_0^2\cdot d_{l1}+P_1\cdot h_1^2\cdot d_{l0})\cdot(P_0+P_1)^2}{P_0\cdot P_1^2\cdot d_{l1}\cdot(h_0+h_1)^2+P_1\cdot P_0^2\cdot d_{l0}\cdot(h_0+h_1)^2}\right]. \tag{18}$$

This result differs from the result obtained by Chu *et al.*, in which the natural lattice constant of the substrate and the layer are assumed to be the same for the calculation of the position of the neutral plane. For thin layers with lattice constants that do not differ significantly from their substrate, this difference can be neglected, but with increasing differences in the lattice constants of the layer and the substrate and with increasing layer thickness, this difference becomes significant. However, an approximation for very thin layers with lattice constants similar to the substrates is

$$R \approx -\frac{h_0^2}{6\cdot d_1\cdot h_1}\cdot\left(1+6\cdot\frac{h_1}{h_0}\right) \tag{19}$$

in agreement with Chu *et al.* (see Appendix B). A further approximation, which would neglect the $(6\cdot h_1/h_0)$ term, results in a similar result as presented by Flinn *et al.*,[17] following a similar energy minimization analysis. Olsen *et al.* presented another approach to the description of the radius of curvature of multilayered heteroepitaxial structures[18,19] but their assumption that the neutral plane always lies in the

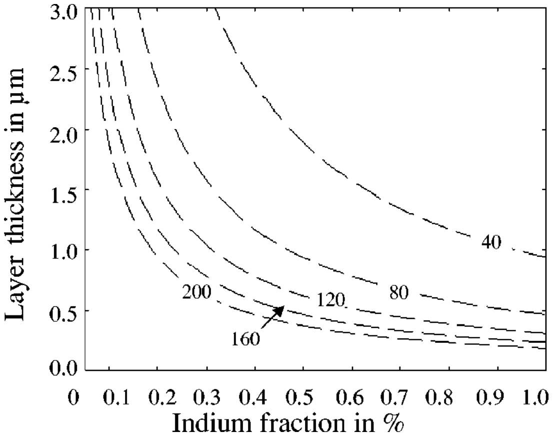

FIG. 4. Contour plot of the radius as a function of the layer thickness and the Indium fraction in the $In_xGa_{1-x}As$ layer on top of a 400-μm GaAs substrate. The labels represent the radius in meters.

middle of the composite is wrong. Figure 4 shows a contour plot of the radius of curvature as a function of the Indium fraction and the layer thickness, and it can be seen that different structures may have the same radius of curvature.

D. Generalization to multilayer systems

For compound structures with more than one layer, the position of the neutral plane and the wafer radius of curvature can be calculated in a similar way as described for the single-layer system. The strain ε_i in the ith layer which is used for the calculation can be found by using Eq. (3) which represents the lattice constant d at the position z. Using d_{li} and ε_i in Eq. (4) this results in

$$\varepsilon_i=\frac{d_{l0}}{d_{li}}\cdot\left(1+\frac{z+h_0-w}{R}\right)-1. \tag{20}$$

For the substrate $i=0$ is used and for successive layers above, $i=1,2,3\ldots$. The forces can be calculated as in Eq. (9) using the appropriate elastic constant and the appropriate strain for each layer and the substrate as

$$F_i=E_i^*\cdot l_w\cdot\int_{z=\left(\sum_{j=1}^{j=i}h_j\right)-h_i}^{z=\sum_{j=1}^{j=i}h_j}\varepsilon_i dz. \tag{21}$$

The position of the neutral plane can then again be found by solving the equation $\Sigma F_i=0$ for w which results in

$$w=\frac{\sum_{i=0}^{i=n}\left[P_i\cdot\left(2\cdot R\cdot d_i-h_i+2\cdot\sum_{j=0}^{j=i}h_j\right)\right]}{2\cdot P}, \tag{22}$$

where n is the total number of layers above the substrate and the following abbreviations were used:

$$P_i=\frac{E_i^*\cdot h_i}{d_{li}},\quad P=\sum_{i=0}^{i=n}P_i\quad\text{and}\quad d_i=1-\frac{d_{li}}{d_{l0}}. \tag{23}$$

The radius of curvature for multi-layered systems can be calculated by solving a generalized equation [Eq. (15)] for each of the layers and the substrate according to

$$W_i=\tfrac{1}{2}\cdot d_{l0}^2\cdot E_i^*\cdot\int_{z=\left(\sum_{j=1}^{j=i}h_j\right)-h_i}^{z=\sum_{j=1}^{j=i}h_j}[\varepsilon_i(z)]^2dz. \tag{24}$$

Using Eq. (22) as an expression for the neutral plane and solving the equation $\partial\Sigma W_i/\partial R=0$ for R leads to the following expression for the radius of curvature:

$$R=-\frac{N}{D}. \tag{25}$$

The numerator (N) and denominator (D) can be expressed as

$$N=\sum_{i=0}^{i=n}\frac{P_i}{d_{li}}\cdot\left\{\frac{1}{12}\cdot h_i^2+\left[\left(\sum_{j=0}^{j=i}h_j\right)-\frac{h_i}{2}-\frac{\sum_{k=0}^{k=n}P_k\cdot\left(\left(\sum_{l=0}^{l=k}h_l\right)-\frac{h_k}{2}\right)}{P}\right]^2\right\}$$

and

$$D=\sum_{i=0}^{i=n}\frac{P_i}{d_{li}}\cdot\left\{\left[\left(\sum_{j=0}^{j=i}h_j\right)-\frac{h_i}{2}\right]\cdot\left(d_i-\frac{\sum_{k=0}^{k=n}P_k\cdot d_k}{P}\right)+d_i\cdot\left[h_0-\frac{\sum_{l=0}^{l=n}P_l\cdot\left[\left(\sum_{m=0}^{m=l}h_m\right)-\frac{h_l}{2}\right]}{P}\right]+\sum_{s=0}^{s=n}P_s\cdot d_s\cdot\left[\frac{\sum_{p=0}^{p=n}P_p\cdot\left[\left(\sum_{r=0}^{r=p}h_r\right)-\frac{h_p}{2}\right]-P\cdot h_0}{P^2}\right]\right\}.$$

Using these equations it is possible to determine the radius of curvature for any layered structure. They also allow the calculation of structures designed to compensate for the radius of curvature, which for example can be achieved by growing a layer with a thickness and lattice constant such that it compensates for the curvature. There are two obvious ways to do this. One is to grow a layer on the same side of the substrate as the initial layer but with the opposite strain. An example would be to grow a GaAsN layer to compensate for the curvature due to an $In_xGa_{1-x}As$ layer grown on a GaAs substrate.

Figure 5 shows the dependence of the radius of curvature on the thickness and on the amount of nitrogen in a compensating GaN_xAs_{1-x} layer grown on top of an $In_{0.005}Ga_{0.995}As$/GaAs structure. The contour line with the

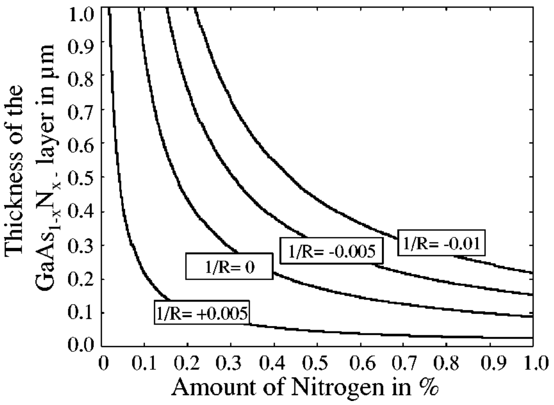

FIG. 5. Contour plots of the radius of curvature R for a 400-μm GaAs substrate, a 0.5-μm In$_{0.005}$Ga$_{0.995}$As layer, and a GaN$_x$As$_{1-x}$ layer on top of the structure. The labels represent the radius in meters.

label "$1/R=0$" indicates the structures for which the curvature has been eliminated. The radius has been calculated using Eq. (25) for a two-layer system and the literature value for the GaN lattice constant,[20] 4.50 Å, has been used. A second way to compensate is to grow an equivalent layer on the back of the substrate. This, however, would require a re-growth procedure, which could well be inconvenient.

III. EXPERIMENTAL RESULTS

The radius of curvature has been determined from different GaAs/ AlAs/ GaAs/ In$_x$Ga$_{1-x}$As samples. The samples (identification numbers S1020999 and S1070999) were grown at the MBE facility at La Trobe University. All samples were grown under As stabilized conditions at a growth rate of approximately 1 ML per second. The GaAs and AlAs layers were grown at a substrate temperature of 600 °C and the In$_x$Ga$_{1-x}$As layer was grown at a temperature of 520 °C. It has been found that the Indium soldering technique commonly used in MBE has a strong impact on the radius of curvature. Therefore the Indium on the back of the samples has been removed using hydrochloric acid. The area where the Indium has diffused into the back of the wafer was successfully removed using a $H_2SO_4:H_2O_2:H_2O$ polishing etchant. The radius of curvature of the structures has been determined using a double crystal x-ray setup, the CuKα_1 line and the (004) reflection from the GaAs substrate. Assuming no (or a uniform) diffusion of the material epitaxially grown on the samples, the Bragg angle of the substrate peak remains constant across the surface. However, in the case of a bent sample the angle between the incident x-ray beam and the (004) plane will depend on the translation position of the sample relative to the beam. Using this dependence the radius of curvature can be determined. The sample was mounted onto a translation stage using double-sided tape on the top edge of the sample to avoid additional strain due to the mounting. After a settling time of about 3 h the sample was found to be stable following relaxation processes in the tape. The sample was then translated to the outermost position where the rocking curve still showed significant intensity from the (004) reflection. The sample was then translated in steps of 2 mm where at every point a rocking curve was collected using the same angular scanning range. The position of the GaAs peaks in each of these rocking curves was then determined by fitting a Gaussian function. From the shift in the peak position with translation the radius of curvature could be determined using the relationship

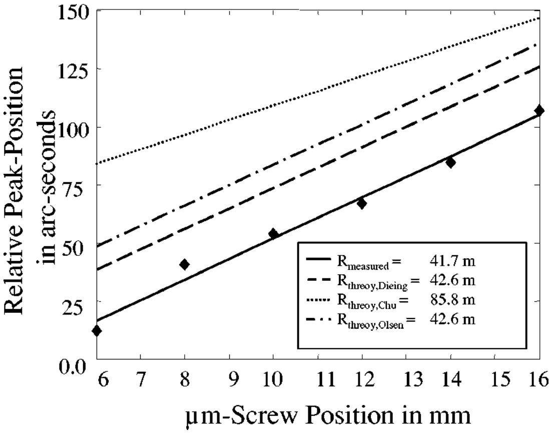

FIG. 6. Theoretical and measured curves for the peak position as a function of the translation of sample S1020999. The measured radius has been determined using a first-order polynomial and a least-square fit.

$$R=\frac{\partial s}{\partial \gamma} \quad \text{or} \quad \frac{1}{R}=\frac{\partial \gamma}{\partial s}, \tag{26}$$

where s is the translation in meters and γ the peak shift in radians.

Figure 6 shows the peak positions of the (004) rocking curves collected from the GaAs substrate of sample S1020999. The sample consists of a 290-μm GaAs substrate (this thickness was determined after the etching), 200-Å AlAs, 200-Å GaAs, and 2-μm In$_{0.002}$Ga$_{0.998}$As. The slope of the upper three lines, which have been offset vertically for clarity, represent the theoretical radius of curvature for the structure calculated using the theory presented here, the theory presented by Olsen and Ettenberg[18,19] and the theory presented by Chu *et al.*[9] As can be seen, the linear fit to the data points used to calculate the radius of curvature fits the theory presented here very well. The difference between the theory presented here, and the solution by Olsen and Ettenberg is $<0.1\%$. However, for structures with larger differences in the elastic properties of their layers the results would differ more significantly. The result obtained from Chu *et al.*'s theory is in significant error, being out by slightly more than a factor of two.

IV. CONCLUSIONS

The theory presented allows calculation of the radius of curvature of a wafer and of the position of the neutral plane for any heterostructure consisting of a substrate and one or more epitaxial layers. The steps necessary to develop expressions for the radius of curvature and the position of the neutral plane are shown in detail. Unlike earlier publications[9,11] this work does not use the formula for the position of the neutral plane originally proposed by Davidenkov[10] for electrolytically deposited materials since that treatment does not include the different strains in the layer(s) and the substrate. Neither does it rely on the equations obtained by Stoney,[7] which cannot be valid for single crystal heterostructures. The present work therefore differs from earlier works and the degree of the differences depends on the thickness and the compositions of the layers in the particular structure of interest. Using the equations above it should now be possible to obtain more detailed and correct information from both *in situ* and *ex situ* wafer curvature measurements.

In the case of a structure consisting of a thin layer positioned at the bottom of the substrate this layer must be assigned the index $i=0$ in the equations above. Since the position of the neutral plane will then be calculated relative to this layer, the radius of curvature, which is calculated relative to the position of the neutral plane, should be corrected. By subtracting the position of the neutral plane (w) from the radius (R) the radius of curvature at the bottom of the lowest layer ($R^*=R-w$) can be calculated. The radius of curvature experimentally determined by collecting rocking curves at different, defined sample positions agrees with the theoretical results very well and therefore supports the theory presented.

ACKNOWLEDGMENTS

Support by the German Academic Exchange Service (DAAD) and Ashland Chemical is gratefully acknowledged. This work has been performed as a part of a dissertation in relation to a degree at the University of Applied Science (NTA) Isny, Germany.

APPENDIX A: APPROXIMATE EXPRESSION FOR THE NEUTRAL PLANE

We start from expression (12) for the position of the neutral plane, which can be approximated by

$$w \approx \frac{h_0}{2} + \frac{E_1^* \cdot h_1 \cdot \frac{1}{d_{l1}} \cdot \left[h_0 + 2 \cdot R \cdot \left(1 - \frac{d_{l1}}{d_{l0}} \right) \right]}{2 \cdot \left(E_0^* \cdot h_0 \frac{1}{d_{l0}} + E_1^* \cdot h_1 \cdot \frac{1}{d_{l1}} \right)}.$$

Here all terms containing h_1^2 that are added to terms involving h_0 were eliminated since $h_0 \gg h_1$. Using Eqs. (17) to simplify terms and substituting R from Eq. (B1) from Appendix B leads to:

$$w \approx \frac{h_0}{2} + \frac{P_1 \left\{ h_0 - 2 \cdot d_1 \cdot \frac{h_0 + h_1}{2 \cdot d_1} \cdot \left[\frac{1}{3} \cdot \frac{(P_0 \cdot h_0^2 \cdot d_{l1}) \cdot (P_0 + 2 \cdot P_0 \cdot P_1)}{P_1 \cdot P_0^2 \cdot d_{l0} \cdot h_0^2} + 1 \right] \right\}}{2 \cdot (P_0 + P_1)}.$$

Once again neglecting h_1 since $h_1 \ll h_0$ this can be simplified even further and after some algebra leads to

$$w \approx \frac{h_0}{2} - \frac{h_0}{6} \cdot \frac{P_0 + 2 \cdot P_1}{P_0 + P_1} \cdot \frac{d_{l1}}{d_{l0}}.$$

Since $h_1 \ll h_0$, then $P_0 + 2 \cdot P_1 \approx P_0 + P_1$ and assuming similar lattice constants leads to

$$w \approx \frac{h_0}{2} - \frac{h_0}{6} = \frac{h_0}{3}.$$

APPENDIX B: APPROXIMATE EXPRESSION FOR THE RADIUS OF CURVATURE

Equation (18) is taken as a starting point for this approximation. All terms containing h_1^2 which are added to terms involving h_0 can be eliminated since $h_0 \gg h_1$. Since P_1 is proportional to h_1 terms containing $P_1 \cdot h_1$ and P_1^2 can be eliminated as well. After some algebra this leads to:

$$R \approx -\frac{h_0 + h_1}{2 \cdot d_1} \cdot \left(\frac{1}{3} \cdot \frac{P_0 \cdot d_{l1}}{P_1 \cdot d_{l0}} + \frac{2 \cdot d_{l1}}{3 \cdot d_{l0}} + 1 \right). \qquad \text{(B1)}$$

By substituting P_0 and P_1, as seen from Eqs. (17), assuming that $E_1^* \approx E_0^*$ and again eliminating h_1^2 terms, leads to

$$R \approx -\frac{h_0 + h_1}{2 \cdot d_1} \cdot \left(\frac{h_0 \cdot d_{l1}^2 + 2 \cdot h_1 \cdot d_{l1} \cdot d_{l0} + 3 \cdot h_1 \cdot d_{l0}^2}{3 \cdot h_1 \cdot d_{l0}^2} \right).$$

Assuming similar lattice constants ($d_{l0} \approx d_{l1}$) this results in

$$R \approx -\frac{h_0^2}{6 \cdot d_1 \cdot h_1} \cdot \left(1 + 6 \cdot \frac{h_1}{h_0} \right). \qquad \text{(B2)}$$

---

*Electronic address: t.dieing@ee.latrobe.edu.au

[1] A. Y. Nikulin, J. R. Davis, and B. Usher, J. Phys. D **33**, 2521 (2000).

[2] J. A. Floro, E. Chanson, S. R.Lee , R. D. Twesten, and R. Q. Hwang, J. Electron. Mater. **26**, 356 (1997).

[3] S. Hearne, E. Chanson, J. Han, J. A. Floro, J. Figiel, J. Hunter, H. Amano, and I. S. T. Tsong, Appl. Phys. Lett. **74**, 356 (1999).

[4] J. Han, J. J. Figiel, M. H. Crawford, and J. A. Floro, in *Proceedings of the Third Symposium on III-V Nitride Materials and Processes* (Third Symposium on III-V Nitride Materials and Processes, Boston, MA, 1999), pp. 137–144.

[5] T. Kozawa, T. Kachi, H. Kano, H. Nagase, N. Koide, and K.

Manabe, J. Appl. Phys. **77**, 4389 (1995).

[6] B. J. Skromme, H. Zhao, D. Wang, H. S. Kong, M. T. Leonard, G. E. Bulmann, and R. J. Molnar, Appl. Phys. Lett. **71**, 829 (1997).

[7] G. G. Stoney, Proc. R. Soc. London, Ser. A **82**, 172 (1909).

[8] I. J. Levinson, *Mechanics of Materials*, 2nd ed. (Prentice-Hall, London, 1970).

[9] S. N. G. Chu, A. T. Macrander, K. E. Strege, and W. D. Johnston, J. Appl. Phys. **57**, 249 (1985).

[10] N. N. Davidenkov, Fiz. Tverd. Tela (Leningrad) **2**, 2919 (1960) [Sov. Phys. Solid State **2**, 2595 (1961)].

[11] I. C. Noyan and A. Segmller, J. Appl. Phys. **60**, 2980 (1986).

[12] P. H. Townsend, D. M. Barnett, and T. A. Brunner, J. Appl. Phys. **62**, 4438 (1987).

[13] S. P. Timoshenko and D. H. Young, *Elements of Strength of Materials*, 5th ed. (D. van Nostrand, Princeton, 1968).

[14] A. S. Hall, *An Introduction to the Mechanics of Solids* (Wiley, Sydney, 1973).

[15] S. Adachi, J. Appl. Phys. **58**, R1 (1985).

[16] W. A. Brantley, J. Appl. Phys. **44**, 534 (1973).

[17] P. A. Flinn, D. S. Gardner, and W. D. Nix, IEEE Trans. Electron Devices **ED-34**, 689 (1987).

[18] G. H. Olsen and M. Ettenberg, J. Appl. Phys. **48**, 2543 (1977).

[19] G. H. Olsen and M. Ettenberg, *Crystal Growth Theory and Techniques* (Plenum, London, 1977).

[20] S. Nakamura and G. Fasol, *The Blue Laser Diode* (Springer, Berlin, 1997).